Defects on TiO_2 (110) surfaces

Madhavan Ramamoorthy, R. D. King-Smith, and David Vanderbilt
Department of Physics and Astronomy, Rutgers University, Piscataway, New Jersey 08855-0849
(Received 20 July 1993)

We present self-consistent *ab-initio* total-energy calculations on TiO_2 (110) surfaces for which the atomic geometry has been relaxed to equilibrium. For stoichiometric supercells we find no surface states in the bulk band gap, in accord with experiment. Oxygen vacancies on the surface give rise to Ti 3*d*-like surface states at the edge of the bulk conduction band. The relaxations of the atoms at the surface were found to be substantial, and those induced by a vacancy were localized in its vicinity. Bulk vacancies introduce states about 0.3 eV below the edge of the bulk conduction band.

I. INTRODUCTION

TiO_2 is a wide band gap semiconductor with a rutile structure. It is a catalyst for the photodissociation of water,[1] and is also used as a support for some transition metal catalysts, where it exhibits a strong metal-support interaction.[2] Hence there is technological motivation to understand the electronic and chemisorption properties of the surfaces of TiO_2. In addition, there has been fundamental interest in understanding the nature of the surfaces of this material, as that of a prototypical transition metal oxide, especially as stoichiometric and ordered surfaces of the (110), (100), and (001) orientations are relatively easy to prepare. These have been studied using a number of high vacuum, surface-sensitive experimental techniques, including low-energy electron diffraction (LEED), electron energy loss spectroscopy (EELS), x-ray photoelectron spectroscopy (XPS), ultraviolet photoelectron spectroscopy (UPS), and inverse photoemission spectroscopy (IPE). The level of understanding of this and other transition metal oxide surfaces, as of 1985, has been summarized by Henrich.[3] The photoemission studies were conducted on slightly reduced samples, with defect levels pinning the Fermi energy (E_f) just below the bulk conduction band minimum. For nearly perfect surfaces giving (1×1) LEED patterns, the dominant feature seen in UPS (Refs. 4–6) is the intense photoemission from the 6 eV broad valence band extending from 3 eV below E_f. The photoemission spectrum was found to be almost independent of surface orientation. The emission in the bulk band gap was found to be negligible, indicating the absence of any surface states with energies in this range.

Oxygen vacancies are induced on TiO_2 (110) by means of ion bombardment or controlled thermal annealing and quenching. These have a marked effect on the electronic properties of the surface, making the sample conducting. A tail of defect states is found in the bulk band gap, indicated by emission from states about 0.8 eV below E_f in UPS,[4–8] EELS,[9] and IPE (Ref. 10) investigations. The chemisorption of small molecules on the (110) surface was found[11] to be strongly affected by the presence of defects. For low densities, the defects are believed to be isolated oxygen vacancies with the defect-induced electronic states localized on the neighboring Ti atoms. Some support for this view comes from XPS studies[12] of the oxygen-deficient surfaces, which indicate that a fraction of the emission from the Ti 2*p* and Ti 3*p* core levels shifts to lower binding energies, relative to that from stoichiometric TiO_2 (110). For a small concentration of defects, the additional peak is shifted by 1.7 eV, which is close to the experimental estimate for stoichiometric Ti_2O_3, where Ti is in the formal +3 oxidation state. However, extensive experimental and theoretical work on bulk TiO_2 (Ref. 13) has indicated that isolated vacancies in reduced rutile are eliminated for deviations from stoichiometry above 10^{-3} by the formation of crystallographic shear planes. Thus, there is interest in a theoretical investigation of models of stoichiometric and defective TiO_2 (110), to determine whether models with isolated bulk or surface vacancies are sufficient to explain the experimental observations. Such an investigation would also set the stage for further work on the chemisorption of metal layers and small molecules on this surface to shed light on the catalytic properties of this material.

Theoretical work on resolving this issue has so far been limited. Previous work on TiO_2 (110) in which the electronic calculation has been carried out to self-consistency, has only been applied to stoichiometric supercells. The forces on the atoms were not calculated, and the coordinates of the atoms were not relaxed to equilibrium. An early investigation by Kasowski and Tait,[14] using the linear muffin-tin orbitals method, focused on the calculation of the electronic density of states of a three-layer stoichiometric supercell with atoms in bulklike positions. They found O 2*p* states in the bulk band gap which were driven below the bulk valence band edge when the topmost oxygen atoms on the surface were relaxed inward by 0.2 Å. Podloucky *et al.*[15] have recently reported a calculation of the electronic structure of three-layer slabs of clean and hydrogenated TiO_2 (110), using the full-potential linearized augmented plane wave method. They relaxed only the topmost oxygen atoms on the surface (by optimizing the total energy of the slab), obtaining an inward relaxation of 0.1 Å and a band gap of 1.0 eV.

Work on the electronic structure of the defective sur-

face has been based on cluster calculations or tight-binding models. Tsukada *et al.*[16] have carried out DV-$X\alpha$ calculations of clusters and find that removing a surface bridging oxygen atom gives rise to a defect level 1.0 eV below the conduction band minimum. Munnix and Schmeits[17] used a tight-binding model to calculate the density of states of stoichiometric and defective (110) supercells. For the stoichiometric supercells they found no states in the band gap, while for the oxygen-deficient supercells they found states in the band gap when oxygen vacancies were present at surface bridging and on subsurface sites. However, they had to adjust the positions of the Ti atoms near the subsurface oxygen vacancy to make the energies of the defect states correspond to those of experimental data. Halley *et al.*[18] calculated the electronic structure of finite blocks of TiO_2, with the atoms in their bulklike arrangements, and a random distribution of oxygen vacancies. They represented the contribution to the electrostatic potential from the defect states approximately by a Yukawa-like potential with a soft core and found a tail of defect states in the band gap which resulted from vacancies on the surface and in the bulk. However, in this work there were several parameters of the approximate potential that were chosen arbitrarily. Wang and Xu[19] have studied stoichiometric and defective supercells of TiO_2 (110) (with atoms in bulklike positions) using a tight-binding extended Huckel method. They find defect states localized around surface Ti atoms when one-half or all the surface bridging oxygen atoms are removed, giving a tail of defect states in the band gap, in rough correspondence with experiment.

In the last few years several advances in computational algorithms and pseudopotential calculations have occurred, making it feasible to carry out first-principle pseudopotential total-energy calculations of transition metal oxide supercells of substantial size. It is of interest to apply these techniques to a simple, nonmagnetic, charge-transfer insulator like TiO_2. Our calculations represent the first attempt to carry out *ab initio* self-consistent total-energy calculations on this system, using these novel approaches. We have studied a number of structures, within the bounds imposed by limitations of computer time and memory, to understand systematically the structural and electronic properties of stoichiometric and oxygen-deficient TiO_2 (110). We find that surface oxygen vacancies indeed give rise to defect states close to the Fermi energy of the sample, and one needs subsurface vacancies to explain some of the tail extending into the bulk band gap. While this was hinted at by the earlier tight-binding calculations, the present work was necessary to put these ideas on a sound footing. As we shall show, the structural relaxations that occur on the stoichiometric and defective surfaces are appreciable. Thus it was not clear *a priori* whether calculations which neglected relaxations, or which put them in by hand, could be trusted.

The plan of the paper is as follows. Section II gives a brief summary of the technique used to carry out the calculations. In Sec. III we give our results for the lattice parameters and vibrational frequencies of bulk TiO_2. In Sec. IV we give a description of the structure of the stoichiometric TiO_2 (110) surface. We follow this up with a description of the structural relaxations of oxygen deficient supercells of the surface and the bulk in Secs. V and VI, respectively. In Sec. VII, we present the picture we obtain for the one-electron spectrum of stoichiometric and oxygen-deficient TiO_2 (110) and compare our results with experimental results. Finally in Sec. VIII we conclude our paper by indicating what light we think our work has shed on the understanding of the properties of this material.

II. CALCULATION METHOD

Self-consistent total-energy pseudopotential calculations were carried out with the electronic wave functions expanded in a plane-wave basis. The core electrons were frozen and the valence electron wave functions, for a given geometry of the ions, were obtained by minimizing the Kohn-Sham total-energy functional. A preconditioned conjugate-gradient minimization approach,[20] based on a modification of the approach of Teter, Payne, and Allan,[21] was used. The exchange and correlation contribution to the total energy was treated using the local-density approximation (LDA) with the Ceperley and Alder form of the exchange correlation potential.[22] The forces on the ions were computed and the ions relaxed towards their equilibrium positions using an iterative modified Broyden technique.[23]

The pseudopotentials for titanium and oxygen were developed using a technique pioneered by Vanderbilt,[24] which permitted the use of a modest cutoff of 25 Ry for the electronic wave functions. The $3s, 3p, 4s$, and $3d$ electrons of titanium were treated as valence electrons, and the pseudopotential was generated in the $3s^2 3p^6 4s^2 3d^1$ configuration. The core radius was taken to be 1.8 a.u. For oxygen, $2s$ and $2p$ levels were treated as valence levels. The reference configuration was $2s^2 2p^4$ with a core of radius 1.3 au. In both cases two reference energies were used per angular momentum channel. This enabled the logarithmic derivative of the pseudo-wave-functions at the core radius to track that of the all-electron wave function over an extensive range of energies. This greatly improved the transferability of the pseudopotential.

III. TESTS ON BULK TiO_2

The pseudopotentials for Ti and O were tested by computing the lattice parameters of bulk rutile TiO_2.[25] The unit cell of this structure is tetragonal and contains two units of TiO_2. The optimal values of the unit cell volume, the ratio of the lengths of the edges c/a and the parameter u (which describes the positions of the oxygen atoms within the unit cell) were obtained through a series of one-dimensional minimizations of the total energies of structures. These values were within 1% of experimental estimates,[26] as indicated in Table I. The accuracy of these results is comparable to that obtained by Allan and Teter,[27] and Glassford and Chelikowsky.[28] The pseudopotentials used were identical to those used by King-

TABLE I. Calculated values of bulk lattice parameters of TiO_2, compared with experiment.

Property	Expt.	Theory[a]	Theory[b]	Theory[c]
cell vol. (Å^3)	62.434	61.161	64.84	62.220
a (Å)	4.594	4.567	4.653	4.584
c/a	0.644	0.642	0.637	0.646
u	0.305	0.307	0.305	0.304

[a]Present calculation.
[b]Glassford and Chelikowsky (Ref. 28).
[c]Allan and Teter (Ref. 27).

Smith and Vanderbilt[29] in an investigation of the ferroelectric properties of $BaTiO_3$. Their calculations gave the lattice constant of the cubic perovskite phase to within 1.5% of experiment. Our success in obtaining the lattice parameters of rutile TiO_2 to high accuracy with these pseudopotentials, with no further optimization, gives an indication of their excellent transferability.

The frequencies of some high-symmetry phonon modes were calculated. These phonon modes correspond to oscillations of the oxygen atoms within the unit cell, with the titanium atoms fixed. The calculated frequencies are given in Table II. The notation used for the vibrational modes and the experimental values quoted were obtained from Traylor *et al.*[31] The agreement of the calculations with experiment is found to be excellent.

The one-electron Kohn-Sham eigenvalues were computed at a number of high symmetry points in the bulk Brillouin zone. A direct band gap of 2.0 eV was found at the Γ point. This underestimation of the band gap, by about 33%, is characteristic of LDA. The details of the band structure are almost identical to those obtained by Glassford and Chelikowsky.[28] They calculated the density of states of the valence and conduction bands and found the widths and qualitative structure of these bands to be in good agreement with experiment. Their work indicates that, apart from the underestimation of the band gap, the LDA gives a realistic picture of the one-electron energy spectrum of bulk TiO_2. Thus, we have made direct comparison of the one-electron eigenvalues with the published experimental spectra.

IV. THE STOICHIOMETRIC TiO_2 (110) SURFACE

The standard model of the stoichiometric TiO_2 (110) surface is given in Fig. 1. The surface has rows of fivefold- and sixfold-coordinated Ti atoms along the bulk [001] direction. These are parallel to rows of threefold-coordinated oxygen atoms lying in the plane of the surface Ti atoms. Rows of twofold-coordinated oxygen atoms (bridging oxygen atoms) are about 1.25 Å above this plane. In an ionic picture of the material, as made up of Ti^{4+} and O^{2-} ions, such a surface would be neutral. From a more covalent point of view, such a cleavage breaks the minimum possible number of bonds.

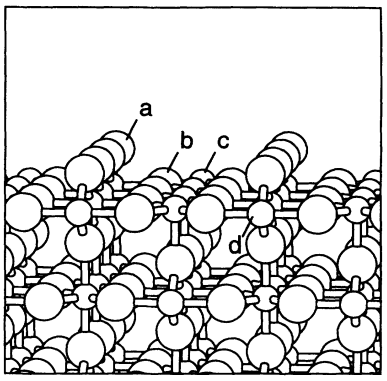

FIG. 1. The structure of the stoichiometric (110) surface of TiO_2. The different types of surface atoms are indicated as follows: (a) bridging oxygen atoms; (b) coplanar oxygen atoms; (c) and (d), surface titanium atoms. Atoms of type (a) and (c) have one less nearest neighbor than in the bulk, while (b) and (d) have the full complement of nearest neighbors.

Three-layer and five-layer slabs of stoichiometric TiO_2 (110), with all the bridging oxygen atoms on the surface present, were relaxed to equilibrium. In the relaxed structure, the force on each ion was smaller than 0.05 eV/Å. The relaxation of the three-layer slab was found to be in quantitative agreement with that of the five-layer slab to within 10%. Convergence of the calculated relaxations and surface energies of the structures with respect to vacuum layer thickness was tested. Two special k points, at the (0.25,0.125,0.25) and (0.25,0.375,0.25) positions in the (1×1) supercell Brillouin zone, were used in the self-consistent total-energy calculation. The surface energy of the three-layer slab differed from that of the five-layer slab by less than 5%.

The relaxed structure of the five-layer slab is given in Fig. 2(a). The surface has a puckered arrangement of atoms with the the sixfold-coordinated Ti atoms and the

TABLE II. Comparison of experimental and calculated values of the frequencies of some zone-center phonon modes.

Label	Expt.[a] (10^{12} Hz)	Theory (10^{12} Hz)
Γ_1^+	18.30±0.46	17.64
Γ_4^+	24.72±0.25	23.73
Γ_3^+	4.246±0.09	4.44
Γ_5^-	13.339±0.18	13.34

[a]Traylor *et al.* (Ref. 31).

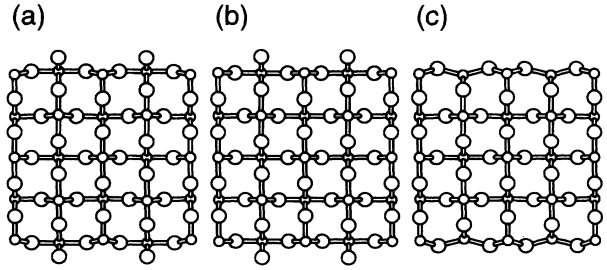

FIG. 2. Side view along the bulk [001] direction of the relaxed five-layer slabs. (a) Relaxed stoichiometric slab; (b) unrelaxed stoichiometric slab; (c) relaxed defective (1×1) slab.

coplanar oxygen atoms moving outward by 0.1 Å. The fivefold-coordinated Ti atoms and the bridging oxygen atoms move inward by approximately the same amount. These relaxations are simply understood in terms of a chemical bonding picture in which the undercoordinated titanium and oxygen atoms on the surface move from their bulklike positions to be closer to their neighbors.

The surface energy of the (110) surface was calculated to be about 1.25 eV per (1×1) surface unit area. This estimate is about two to three times larger than the experimental values compiled in the review of Overbury *et al.*[30] The experiments were conducted at temperatures above 2500 K and the comparison with our ground state calculations on ideal, ordered structures is rather tenuous. An alternative model of the stoichiometric surface has, instead of bridging oxygen atoms, rows of onefold-coordinated oxygen atoms about 2 Å above rows of sixfold-coordinated Ti atoms. This model would leave one-half of the surface Ti atoms only fourfold-coordinated. Our calculations estimated the surface energy of this model was about 4.1 eV per (1×1) surface unit, appreciably higher than that of the standard model.

V. OXYGEN DEFICIENT TiO_2 (110)

As discussed in the Introduction, there have been extensive experimental investigations of the effect of oxygen deficiency on the electronic structure and chemical reactivity of the surfaces of TiO_2. This motivated our interest in studying nonstoichiometric slabs of TiO_2 (110). Slab geometries composed of from three to five layers, with all or part of the bridging oxygen atoms removed from the surface, were relaxed to equilibrium. It should be emphasized that we removed neutral oxygen atoms from the model surfaces, and not O^{2-} ions. Thus, for each oxygen atom removed, two electrons are found to remain on the surface, occupying nonbonding, 3*d*-like levels localized primarily on the surface Ti atoms. (These levels were not separated by a gap from the conduction band levels.) Thus, the surfaces that we studied were all electrically neutral.

The relaxed structure of the five-layer oxygen-deficient (1×1) slab is given in Fig. 2(c). The surface contains fivefold-coordinated Ti atoms which move inward by 0.05 Å and fourfold-coordinated Ti atoms which move in by 0.13 Å. The coplanar oxygen atoms move dramatically outward by 0.35 Å, indicating a marked deviation of the valence orbitals on these atoms from the planar sp^2-like hybridization present in bulk TiO_2. Again, the relaxation of the three-layer slab was found to be in quantitative agreement with that of the five-layer slab to within 10%. Surface energies, too, were converged to within 5%.

Since the (1×1) structures with all surface bridging oxygen atoms missing is not likely to be a realistic model of the experimental sample, we endeavored to study supercells with a lower defect density. The choice of a high defect density (to obtain a smaller surface unit cell) and limited slab thickness was dictated by limitations of computational time and memory. Our experience with the stoichiometric and defective three and five-layer (1×1) supercells indicated that structural relaxations and surface energies were given rather accurately by three-layer structures. Hence, we focused our attention on three-layer (1×2) and (2×1) supercells, for which only one-half of the bridging oxygen atoms are absent. There was also some motivation for this study from experimental literature,[32,33] where there is mention of a (2×1) structure seen on thermally annealed samples. The possibility that this was a structure with an ordered array of surface oxygen vacancies was worth testing. In addition, the work of Eriksen and Egdell[9] indicates that on creating oxygen deficient surfaces of TiO_2 by controlled electron bombardment, a limiting composition of Ti_4O_7 is reached.

The (1×2) structure simulated had alternate bridging oxygen atoms missing along each row, while the (2×1) structure had alternate rows of bridging oxygen atoms missing. The configuration of bonds on the two surfaces is rather different. On the (2×1) surface all Ti atoms below the row of oxygen vacancies are only fourfold-coordinated, with the bonding of the other Ti atoms on the surface unchanged. These fourfold-coordinated Ti atoms relax inward by 0.2 Å. For the (1×2) surface, on the other hand, every Ti atom that is bonded to a bridging oxygen atom is fivefold coordinated. In the relaxed structure these are displaced along the [001] direction away from the neighboring vacancy by 0.1 Å, with negligible relaxation along the surface normal. The relaxations of the other surface atoms on both of these structures were found to be almost identical.

In the vicinity of the bridging oxygen atoms, the relaxations were nearly indistinguishable from those of the stoichiometric surface. Near a vacancy the relaxations of the coplanar oxygen atoms was found to be outward and of magnitude 0.3 Å in both structures, rather close to that on the defective (1×1) surface. This indicates that the relaxation induced by surface oxygen vacancies is rather localized. Of the two structures, the (1×2) structure was found to be lower in energy than the (2×1) by about 0.13 eV per (1×1) surface unit area. This surface energy difference is rather small compared to the total surface energy of each of these structures. These calculations suggest that the (2×1) LEED pattern reported occasionally in experimental literature might arise from a more complex structure than the one we have studied.

The relative stability of surfaces of different stoichiometry may be discussed using the grand thermodynamic potential, defined as

$$\Omega = E - \mu_O N_O - \mu_{Ti} N_{Ti} , \qquad (1)$$

where E, N_O, and N_{Ti} are the total energy, number of O atoms, and number of Ti atoms, respectively, in the surface slab geometry considered. As each surface is in equilibrium with the bulk, the chemical potentials μ_{Ti} and μ_O are constrained such that $\mu_{Ti} + 2\mu_O$ is equal to the energy of the bulk per TiO_2 unit. The residual degree of freedom, $\mu_{Ti} - \mu_O$, is constrained to lie in the range

$$\mu_{Ti(bulk)} - \Delta H_f - \mu_{O(gas)} \leq \mu_{Ti} - \mu_O \leq \mu_{Ti(bulk)} + \tfrac{1}{2}\Delta H_f - \mu_{O(gas)} , \qquad (2)$$

where $\mu_{Ti(bulk)}$ and $\mu_{O(gas)}$ are the energies per atom of bulk Ti and molecular O_2, respectively, and ΔH_f is the heat of formation of bulk TiO_2. This follows from the condition that neither bulk Ti nor molecular O_2 should be precipitated. Such considerations have been discussed in detail by Qian *et al.*[34] and Northrup[35] in their studies of GaAs surfaces. In our calculations we have difficulty fixing the limits accurately, as our codes are not currently capable of the careful Fermi-surface sampling and spin polarization needed for bulk Ti and O_2, respectively. Using experimental values for $\mu_{Ti(bulk)}$, $\mu_{O(gas)}$, and ΔH_f, we estimate that the stoichiometric surface should remain stable with respect to the oxygen-deficient ones over the entire accessible range of μ_O. However, the uncertainties are too large to be sure of this conclusion near the lower limit of μ_O.

Some stability considerations are independent of the detailed knowledge of the range of chemical potentials, as they involve comparing surfaces with the same density of surface oxygen atoms. The stability of the (1×2) slab over the (2×1) slab, discussed above, is one such case. Another example is the stability of the (1×2) and (2×1) structures individually against phase separation into two domains of equal area, one with all the bridging oxygen atoms present and the other with all the bridging oxygen atoms missing. To answer this question we compare the surface energy of each of the (1×2) and (2×1) slabs with the average of the surface energies of the stoichiometric (1×1) and defective (1×1) surfaces. In both cases, we find that the surface with only half of the bridging oxygen atoms present is stable with respect to phase separation.

VI. OXYGEN DEFICIENT BULK TiO_2

To obtain further insight into the effects of oxygen vacancies on the electronic structure of the material, we studied a bulklike defective supercell. A bulk supercell with four units of TiO_2 was set up. This was identical in geometry with the (1×2) surface slab, but without the vacuum layer, and with the top and bottom layers identified. The lattice vectors of this supercell were along the bulk [110], [1$\bar{1}$0], and [001] directions with the length doubled along the [001] direction. One oxygen atom in the central layer of this supercell was removed, leaving the three Ti atoms to which it was bonded five-fold coordinated. Of these Ti atoms, the two along the [001] direction relaxed in opposite directions by 0.1 Å. This is almost identical to the relaxations near a vacancy in the (1×2) surface slab. However, the relaxations of the neighboring oxygen atoms were much less dramatic in the bulk, as compared with those on the surface slabs. In the former case, all the oxygen atoms are threefold coordinated, while in the latter, the twofold-coordinated bridging oxygen atoms on the surface are free to relax outward substantially.

VII. ELECTRONIC BAND STRUCTURE OF TiO_2 (110)

The electronic band structure of the stoichiometric and the reduced five-layer slabs are given in Fig. 3. The bands

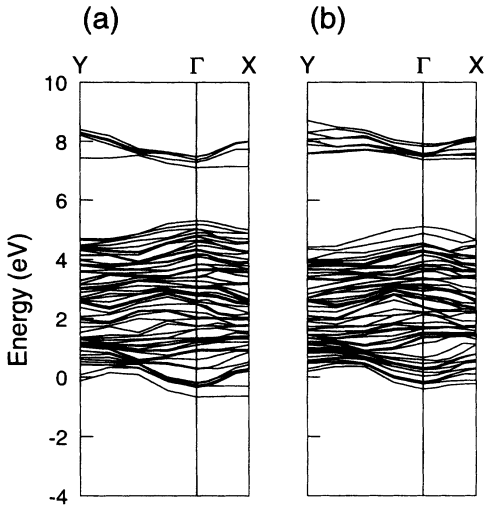

FIG. 3. The electronic band structure of the relaxed (1×1) slabs along the axes of the surface Brillouin zone. (a) Stoichiometric; (b) reduced.

of the different slabs were aligned with respect to each other using the average potential in a layer at the center of each slab. A comparison of the energies of the Ti 3*p* levels localized around each of the two Ti atoms in this region indicates the accuracy with which the potential distribution in this region is representative of the bulk. In an infinitely thick slab, these energy levels should be identical. However, for the three-layer stoichiometric slab, the average of the Ti 3*p* energies on these atoms is split by 1.1 eV. In the five-layer stoichiometric slab, the splitting is reduced to 0.37 eV. For the reduced surface, the corresponding values for the three-layer slab and five-layer slabs are 0.42 and 0.16 eV, respectively. Thus, even the thickest slabs that we have studied probably do not have a completely bulklike potential distribution in the central layer. This is bound to have an effect on the electronic structure. An additional complication is that the lowest conduction band levels of the stoichiometric slab are bulklike, while those in the reduced slabs are highly localized on the surface layer. Thus, these states are affected differently in these two slabs. To reduce the errors in comparing energy levels of valence and conduction bands from different supercells, we have compared the electronic structure of the surface slabs with each other, on the one hand, and the electronic structure of the bulk defective supercell with a perfect bulk supercell, on the other.

In the reduced slab, there are occupied states at the edge of the bulk conduction band, which are localized mainly around the surface Ti atoms. There is no gap between these states and the low-lying unoccupied Ti 3*d* states. Also the gap between these defect levels and the highest occupied O 2*p* levels is significantly wider than that of the bulk, owing both to a depletion of O 2*p* bands at the top of the valence band, and also to an upward shift of the surface defect state energies on the reduced surface, with respect to the bulk conduction band edge. This indicates that our slabs are not thick enough to

TABLE III. The valence and conduction band edges of the various (110) supercells.

	Layers	E_V	E_C
Stoichiometric (1×1)	3	5.63	7.11
Stoichiometric (1×1)	5	5.31	7.10
Defective (1×1)	3	5.01	7.43
Defective (1×1)	5	5.10	7.38
Defective (1×2)	3	4.90	7.38
Defective (2×1)	3	5.49	7.41

describe the bulk, as the widening of the gap of an infinite slab is impossible. The electronic structure of the (1×2) and (2×1) slabs has also been calculated along some high symmetry directions. Table III gives the energies of the highest O $2p$ level and the lowest Ti $3d$ level (occupied in a defective slab) for various (110) supercells. It is seen that for all the defective slabs, the lowest occupied Ti $3d$ level is shifted about 0.3 eV above the bulk conduction band minimum.

When the electronic structure of the bulk supercell containing an oxygen vacancy is aligned with the perfect bulk supercell, it is found that the defect states are 0.3 eV below the bulk conduction band minimum. Table IV gives the energies of the highest O $2p$ level and the lowest Ti $3d$ level (occupied in a defective slab). Once again no gap is found between the defect levels and the unoccupied conduction band levels.

The electronic levels of the stoichiometric and oxygen-deficient structures indicate that the defect levels arising from surface oxygen vacancies lie about 0.3 eV above the bulk conduction band edge, while those due to bulk vacancies lie about 0.3 eV below it. Thus, on a disordered TiO_2 (110) surface comprising a mix of stoichiometric and reduced regions, the Fermi level will be pinned at different energy positions in the different regions. In order to equilibrate the chemical potential throughout the surface, there would be a flow of electrons from the reduced surface patches to the adjoining bulk and stoichiometric surface regions, giving rise to dipole layers at the interfaces between patches. Thus, levels detected in surface spectroscopies up to 0.25 eV below E_f could be due to occupied Ti $3d$ like conduction band states from stoichiometric regions adjoining the reduced patches on the surface.

Vacancies several layers below the surface may also give rise to emission seen up to 0.5 eV below E_f, if they are realistically modeled by our bulk vacancy calculation. However, the tail of defect states seen 0.8 to 1.0 eV below E_f in photoemission studies, may indicate the existence of more complex defect configurations. Significant local alterations of the structure around vacancy complexes cannot be ruled out, given the fact that even small concentrations of vacancies in bulk TiO_2 are eliminated by the formation of crystallographic shear planes. It would be worthwhile to look at defect configurations which resemble those found in the sheared substoichiometric bulk material, to understand the energetics and the spectroscopic signature of such a dramatic transformation of the surface from the ideal model of the surface.

TABLE IV. The valence and conduction band edges of the bulklike supercells.

	Atoms	E_V	E_C
Bulklike supercell	24	-5.15	-3.34
Defective supercell	23	-5.46	-3.59

VIII. CONCLUSIONS

We have studied a number of supercells to model surface and subsurface oxygen vacancies on TiO_2 (110). The defect configurations that we have studied are rather unrealistic from the experimental point of view, due to memory and computational limitations. However, some trends regarding the structural relaxations around an oxygen vacancy seem to be common to a variety of structures that we have studied. While no direct experimental data on the structure of stoichiometric or defective TiO_2 (110) exists, the structural relaxations that we find in our model structures are substantial. These are within the limit of resolution of LEED and medium energy ion scattering experiments. We find that surface oxygen vacancies give rise to defect states close to the Fermi energy, while bulk vacancies appear to give rise to states within 0.5 eV of E_f.

Further work on larger supercells, combining bulk and surface vacancies, is needed to accurately resolve the energy estimates given above. Supercells with seven or nine layers of titanium atoms may give a potential distribution in the central layer that is more like that found in the bulk material. This would make comparisons of the band structure of different slabs using the average potential in the central layer of the slabs more accurate. Also it would reduce the shifting and splitting of groups of states owing to the reflection of Bloch-like states by the surfaces of the slab. The use of supercells with larger surface unit cells would enable a more accurate simulation of a localized surface and of a subsurface vacancy.

The results presented here are likely to be of interest in fundamental studies aimed at understanding the nature of structural relaxations near oxygen vacancies in transition metal oxides and of the defect levels which might have a dramatic effect on the transport properties and chemical reactivity of the material. Studies of chemisorption of metals on TiO_2 surfaces may also build on these calculations.

ACKNOWLEDGMENTS

This work was supported by NSF MRG Grant No. DMR-89-07553. Cray YMP time was provided by the National Center for Supercomputing Applications under Grant No. DMR920003N. We acknowledge useful discussions with K. W. Kwak, X. Li, F. Liu, R. Nunes, T. Madey, U. Diebold, A. K. See, and R. Bartynski. The assistance of T. A. Pfannkoch with the use of departmental work station facilities is also gratefully acknowledged.

[1] A. Fujishima and K. Honda, Nature **238**, 37 (1972).
[2] G.L. Haller and D.E. Resasco, Adv. Cat. **36**, 173 (1989).
[3] V.E. Henrich, Rep. Prog. Phys. **48**, 1481 (1985).
[4] V.E. Henrich, G. Dresselhaus, and H.J. Zeiger, Phys. Rev. Lett. **36**, 1335 (1976).
[5] Y.W. Chung, W.J. Lo, and G.A. Somorjai, Surf. Sci. **64**, 588 (1977).
[6] R.H. Tait and R.V. Kasowski, Phys. Rev. B **20**, 5178 (1979).
[7] V.E. Henrich and R.L. Kurtz, Phys. Rev. B **23**, 6280 (1981).
[8] R.G. Egdell, S. Eriksen, and W.R. Flavell, Solid State Commun. **60**, 835 (1986).
[9] S. Eriksen and R.G. Egdell, Surf. Sci. **180**, 263 (1987).
[10] A.K. See and R.A. Bartynski, J. Vac. Sci. Technol. A **10**, 2591 (1992).
[11] W. Gopel, G. Rocker, and R. Feierabend, Phys. Rev. B **28**, 3427 (1983).
[12] W. Gopel *et al.*, Surf. Sci. **139**, 333 (1984).
[13] C.R.A. Catlow and R. James, Nature **272**, 603 (1978).
[14] R.V. Kasowski and R.H. Tait, Phys. Rev. B **20**, 5168 (1979).
[15] R. Podloucky, S.G. Steinemann, and A.J. Freeman, New. J. Chem. **16**, 1139 (1992).
[16] M. Tsukada, H. Adachi, and C. Satoko, Prog. Surf. Sci. **14**, 113 (1983).
[17] S. Munnix and M. Schmeits, Phys. Rev. B **31**, 3369 (1985).
[18] J.W. Halley, M.T. Michalewicz, and N. Tit, Phys. Rev. B **41**, 10 165 (1990).
[19] C.R. Wang and Y.S. Xu, Surf. Sci. **219**, L537 (1989).
[20] R.D. King-Smith and D. Vanderbilt, Phys. Rev. B **49**, 5828 (1994).
[21] M. Teter, M. Payne, and D. Allan, Phys. Rev. B **40**, 12 255 (1989).
[22] D.M. Ceperley and B.J. Alder, Phys. Rev. Lett. **45**, 566 (1980).
[23] D. Vanderbilt and S.G. Louie, Phys. Rev. B **30**, 6118 (1984).
[24] D. Vanderbilt, Phys. Rev. B **41**, 7892 (1990).
[25] R.W.G. Wyckoff, *Crystal Structures* (Interscience, New York, 1960), Vol. 1, Chap. IV, p. 7, Table IV, 1.
[26] S.C. Abrahams and J.L. Bernstein, J. Chem. Phys. **55**, 3206 (1971).
[27] D.C. Allan and M.P. Teter, J. Am. Ceram. Soc. **73**, 3247 (1990).
[28] K.M. Glassford and J.R. Chelikowsky, Phys. Rev. B **46**, 1284 (1992).
[29] R.D. King-Smith and D. Vanderbilt, Ferroelectrics **136**, 85 (1992).
[30] S.H. Overbury, P.A. Bertrand, and G.A. Somorjai, Chem. Rev. **75**, 547 (1975).
[31] J.G. Traylor, H.G. Smith, R.M. Nicklow, and M.K. Wilkinson, Phys. Rev. B **3**, 3457 (1971).
[32] C.C. Kao, S.C. Tsai, M.K. Bahl, Y.W. Chung, and W.J. Lo, Surf. Sci. **95**, 1 (1980).
[33] P.J. Moller and M.C. Wu, Surf. Sci. **224**, 265 (1989).
[34] Guo-Xin Qian, R.M. Martin, and D.J. Chadi, Phys. Rev. B **38**, 7649 (1988).
[35] J.E. Northrup, Phys. Rev. Lett. **62**, 2487 (1989).